Wavelet-Based Algorithm for Fault Detection and Discrimination in UPFC-Compensated Multiterminal Transmission Network

J. Pardha Saradhi, R. Srinivasarao, and V. Ganesh

Abstract As interconnected power system transmission line systems are more complex in evaluating system performance, and adding FACTS devices in the power system requires more attention in the analysis. Nowadays FACTS devices play a major role in improving the performance of transmission lines. The evaluation of dynamic behavior during transient conditions is becoming a great difficulty, particularly, for larger networks. Wavelet analysis will give the entire system performance at any part of the system. This paper mainly concentrates on fault detection and its classification of multiterminal networks. It also gives a critical evaluation of nine zones of performance under different fault conditions. Wavelet-based analysis in the presence of UPFC (unified power flow controller) by using Bior 1.5 has been performed. The performance of multiterminal transmission networks with and without controllers under different fault conditions has been estimated.

Keywords FACTS · Wavelet · UPFC · Bior 1.5

J. Pardha Saradhi (✉)
Department of Electrical & Electronics Engineering, Bapatla Engineering College, Bapatla, India
e-mail: pardhasaradhi.jpalli@gmail.com

R. Srinivasarao
Department of Electrical & Electronics Engineering, JNTU, Kakinada, India
e-mail: srinivas.jntueee@gmail.com

V. Ganesh
Department of Electrical & Electronics Engineering, JNTUACEP, Pulivendula, India
e-mail: ganivg@gmail.com

M. N. Favorskaya et al. (eds.), *Innovations in Electrical and Electronic Engineering*,
Lecture Notes in Electrical Engineering 661, https://doi.org/10.1007/978-981-15-4692-1_7

1 Introduction

Because of environmental and energy concerns it is very difficult to construct new transmission lines and generation. So instead of constructing new systems, it is essential to increase power transfer capability using existing systems. In order to meet the needs of power transfer it is more important to control the power flow in transmission lines. In addition to this, FACTS devices play a major role in the transmission system. As they are utilized to control the power flow and to change power system parameters. The parameters like line impedances, bus voltages, and phase angles of the power system can be regulated by means of using FACTS devices such as STATCOM, SVC, SSSC, and UPFC. FACTS devices also have the ability to decrease the generation cost, increasing transmission capacities, and improve the stability and security of power systems. The transient and steady-state components of voltage and current signals are affected by compensating devices during fault conditions. These signals will create problems with relay functioning.

The identification and classification of transmission line faults with FACTS devices is a very difficult task. In [1], current and voltage signals are used to find the fault location. But the fault type and the phase in which fault occurs are not reported. In [2], an adaptive Kalman filtering approach is proposed for protecting uncompensated power distribution networks. In [3], an advanced series compensators for compensated transmission systems is employed. But the limitation Kalman filtering is the requirement of a number of different filters to complete the task and also the fault resistance cannot be modeled. Neural networks are applied in [3–5] for pattern recognition but they need large training time and large data and design of a new neural network are needed for each transmission line. In [1–5] different methods based on support vector machines fuzzy logic systems, TT transform, S transform, and wavelet transform are proposed. In these attempts the classification and identification of faulted section is done in a transmission line compensated by TCSC protected by metal-oxide varistor (MOV) or transmission line compensated by series capacitors protected by metal-oxide varistor (MOV) or compensated by both the above-mentioned approaches. The advantage of post fault current and voltage samples are taken from both ends of the line and build a recursive optimization algorithm to identify the fault distance in a transmission line with a series FACTS device. But there is no need of the FACTS device model in this algorithm and it can able to locate the fault without mentioning the type of fault.

According to [6] Power quality conditions and the impact of FACTS devices can be analyzed by using wavelet analysis more effectively. In [7] fault identification in the presence of FACTS devices is obtained by using fuzzy wavelet approach. In [8], wavelet-based entropy algorithm method is applied to find the fault in the presence of FACTS devices has been discussed, the effectiveness of the wavelet entropy algorithm has been checked. In [9], protective gear response is analyzed by using wavelets, which have been discussed.

The UPFC consists of both STATCOM and SSSC which are connected with a common DC link, which allows the bidirectional flow of real power between series output terminals of SSSC and the shunt terminals of the STATCOM. This work performed with UPFC. Protective schemes design in presence of multiterminal network with UPFC is more difficult nowadays. This paper uses Bior 1.5 as a mother wavelet to perform both fault identification and compensation evaluation in the presence of UPFC.

2 Wavelet Transform

A wavelet analysis is nothing but the expansion of functions by means of wavelets, which are created in the form of dilations and translations of a fixed function known as mother wavelet. A mother wavelet is an oscillatory function which has some finite energy and zero average value. It is possible to obtain time and frequency information of a signal using wavelet transform when compared with fourier transformation, which can give only frequency information.

Wavelet transform provides an effective time-frequency representation of signals. All basis functions are formed by shifting and scaling of "mother" wavelet function $\psi(t) \in L^2(R)$

$$\psi_{m,n}(t) = 2^{-\frac{m}{2}} \psi\left(2^{-m}t - n\right)m, n \in Z \tag{1}$$

Signal $f(t) \in L^2(R)$ can be then represented as

$$f(t) = \sum_m \sum_n d_{m,n} \psi_{m,n}(t) \tag{2}$$

where $d_{m,n}$ are spectral wavelet coefficients

$$d_{m,n} = \left\langle f(t), \psi_{m,n}(t) \right\rangle \tag{3}$$

For discrete signals $f(k) \in L^2(Z)$ gives similar results and its equivalent transform is called Discrete Wavelet Transform (DWT).

3 Flowchart for Fault Identification

3.1 Algorithm

Step 1: Initiate I_{a1}, I_{b1}, I_{c1} … I_{a9}, I_{b9}, I_{c9} at all zones.
Step 2: Obtain detailed coefficients at each bus number 1, 2, 3, 4, 5, 6, and 7.

Step 3: Obtain fault index value at each Bus.
Step 4: Highest values fault index in the zone indicate the fault in that Zone.
Step 5: Highest Value in the particular phase will give the faulty phase where Fault occurs.

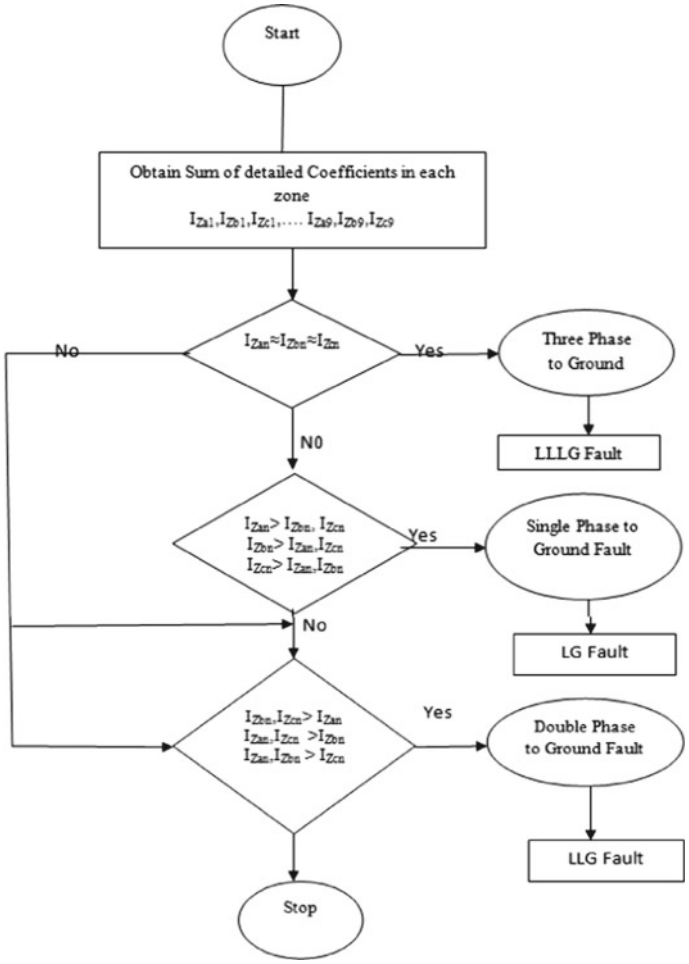

Fig. 1 Flow chart for fault identification

3.2 Flow Chart

4 Test System

4.1 Test System Data and Its Associated Parameters

5 Simulation Results and Analysis

The test system consists of nine zones and seven buses. The length of each zone is shown in the figure. It has five number of DG s and two number of utility grid sources connected. The proposed multiterminal system is operated with 220 kV, 50 Hz. The behaviour of the system is analyzed by using Bior 1.5 mother wavelet detailed coefficients has been calculated and then some of the detailed coefficients have been obtained. Fault analysis carried with the help of wavelet multiresolution analysis for the proposed system with and without UPFC. The performance of the system is studied during line to Ground (LG), Line-Line to Ground (LLG) and Line-Line-Line to Ground Fault (LLLG) at each zone. Coefficients are drawn and tabulated at each bus. Variation of fault index in each bus has analyzed. The analysis also made for different fault inception angles (FIA) and at different distances.

Network during LG Fault in Zone-2, as it has 25 km length, fault analysis has done at different distances and for different fault inception angles. From Table 3 it

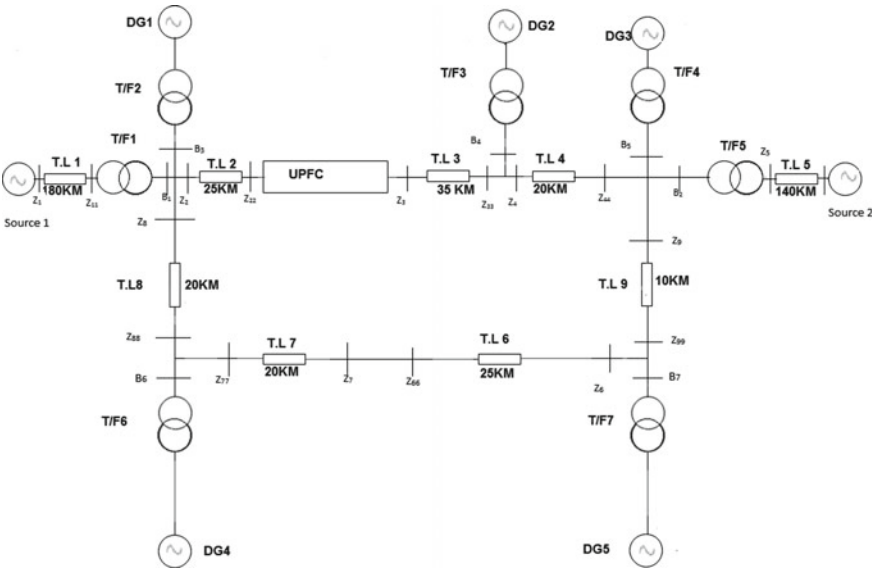

Fig. 2 One line diagram of a test system

Table 1 Test system data

Description	System parameters
Source of supply	**Source 1**: Rated voltage (Vrms) = 400 kV; phase angle of phase A (degrees): 20.2; 3-phase short-circuit level at base voltage(VA): 900 MVA, X/R ratio: 10
	Source 2: Rated voltage (Vrms) = 400 kV; phase angle of phase A (degrees): 20.2; 3-phase short-circuit level at base voltage (VA): 900 MVA, X/R ratio: 10
Distributed generators (DG)	**Generator (DG1)**: Rated power = 189 MVA Line-to-line voltage = 33 kV
	Generator (DG2): Rated power = 50 MVA Rated voltage (Vrms) = 33 kV
	Generator (DG3): Rated power = 200 MVA Rated voltage (Vrms) = 110 kV
	Generator (DG4): Rated power = 200 MVA Rated voltage (Vrms) = 110 kV
	Generator (DG5): Rated power = 150 MVA Rated voltage (Vrms) = 33 kV
Transformer	**Transformer 1**: Nominal power = 900 MVA 400/220 kV
	Transformer 2: Rated power = 200 MVA 33/220 kV
	Transformer 3: Rated power = 100 MVA 33/220 kV
	Transformer 4: Rated power = 100 MVA 33/220 kV
	Transformer 5: Rated power = 200 MVA 400/220 kV
	Transformer 6: Rated power = 200 MVA 110/220 kV
	Transformer 7: Rated power = 150 MVA 33/220 kV
Loads	Load 1: 100 MW Load 2: 25 MW Load 3: 125 MW Load 4: 200 MW Load 5: 100 MW

Table 2 Wavelet information and its associated parameters

Mother wavelet	Bior 1.5
Analyzed information	Detailed coefficients of currents at each bus and zones
Sampling frequency	180 kHz
Actual frequency	50 Hz
Number of samples for cycle	3600

Table 3 LG Fault on Transmission line in Zone-2 without UPFC

FIA		20°	40°	60°	80°
Zones/Phases	Distance (km)				
Zone-1: Phase a	36	1338.427	1342.89	1269.112	1218.884
	72	904.6976	891.4416	935.5863	942.6535
	108	1011.985	943.1618	956.172	940.1689
	144	982.827	838.4148	836.1602	764.5347
	180	921.3867	707.8778	711.8673	644.8466
Zone-1: Phase b	36	1289.998	1295.932	1250.634	1236.385
	72	899.4311	895.4739	804.5511	923.5474
	108	967.2835	947.2077	825.1693	921.0753
	144	938.1209	842.4705	705.167	745.4413
	180	876.7148	711.9523	580.876	553.6225
Zone-1: Phase c	36	181.0136	140.0609	138.8364	148.4208
	72	180.9751	140.0552	138.8456	148.3838
	108	180.944	139.9693	138.7754	148.3702
	144	180.9424	139.9916	138.8042	148.3896
	180	180.8912	139.9425	138.7891	148.3927
Zone-2: Phase a	5	5325.777	5942.902	6243.144	5881.985
	10	5286.246	5137.983	5927.662	6138.758
	15	4267.901	4297.411	5157.559	5000.209
	20	4161.902	4134.042	4384.349	4342.504
	25	3714.04	4040.369	4301.715	4074.849
Zone-2: Phase b	5	602.9014	532.8588	545.8582	520.0408
	10	403.5135	301.5525	280.0188	237.335
	15	226.4366	237.8998	189.8426	162.5452
	20	324.162	227.6833	103.7549	103.3488
	25	313.8367	362.1852	292.0248	357.6616
Zone-2: Phase c	5	609.0574	532.6295	554.8663	533.1901
	10	410.0847	306.9752	265.8487	243.2796
	15	241.3625	244.8704	192.8621	145.0435
	20	323.5173	223.5398	102.1582	102.1004
	25	313.1021	359.939	284.5708	354.1224
Zone-3: Phase a	4	232.0681	156.3246	190.3034	141.1947
	8	360.2451	296.6683	273.1152	199.9896
	12	302.7981	237.6175	167.804	148.7093
	16	690.8967	523.5822	389.8835	319.3736
	20	502.1092	769.6736	657.1128	706.9336

(continued)

Table 3 (continued)

FIA		20°	40°	60°	80°
Zones/Phases	Distance (km)				
Zone-3: Phase b	4	88.58852	104.1699	64.67646	52.09059
	8	109.1919	110.9402	115.9707	120.0759
	12	115.2178	136.103	146.1664	160.5939
	16	238.9	179.2664	175.1665	194.2011
	20	321.4526	342.6262	281.8157	314.3333
Zone-3: Phase c	4	83.82115	104.6752	60.75328	47.86299
	8	110.8297	110.1213	120.3456	122.1523
	12	120.4266	137.1244	143.6077	157.0114
	16	238.5705	180.0519	173.4791	192.4714
	20	329.9034	345.9209	290.1367	317.3911
Zone-4: Phase a	7	532.6241	348.9311	306.3755	231.5944
	14	453.5099	436.2159	401.0555	414.4105
	21	504.0367	374.652	220.8545	263.5287
	28	504.1185	460.9027	390.3962	270.782
	35	470.6284	457.345	489.7008	459.9936
Zone-4: Phase b	7	116.3134	95.57828	84.63895	95.03919
	14	157.872	99.26329	140.6984	161.0165
	21	193.4907	214.9099	198.6255	113.5626
	28	181.0133	177.6535	193.5296	246.8691
	35	469.7538	417.0691	341.1754	321.499
Zone-4: Phase c	7	112.0267	95.78919	88.52096	99.66043
	14	150.6757	96.09216	129.4061	153.7648
	21	176.6552	199.805	184.1064	92.92766
	28	167.3412	173.1193	188.3263	247.5583
	35	473.4147	411.2601	356.2149	326.3267
Zone-5: Phase a	28	385.0973	431.6954	424.9349	421.1367
	56	352.2491	397.267	379.3608	376.8893
	84	323.4669	372.754	362.7732	371.6509
	112	288.2593	333.1941	357.6824	377.2478
	140	289.3428	308.4371	348.8621	371.407
Zone-5: Phase b	28	452.928	514.9861	403.4833	465.1621
	56	423.5847	480.5515	383.8425	446.8402
	84	391.2431	456.0335	374.2237	448.576
	112	357.3886	420.3918	359.4948	440.6106
	140	338.5571	391.7091	330.9635	418.9813

(continued)

Table 3 (continued)

FIA		20°	40°	60°	80°
Zones/Phases	Distance (km)				
Zone-5: Phase c	28	151.6729	102.0236	56.68258	116.5944
	56	151.6744	102.0308	56.68669	116.589
	84	151.6738	102.0231	56.68036	116.5966
	112	151.6677	102.0247	56.68228	116.5964
	140	151.6595	102.0238	56.68666	116.6045
Zone-6: Phase a	5	355.8378	284.2098	308.5839	302.9133
	10	509.6473	387.7858	376.2189	351.3724
	15	481.2672	446.2837	371.9514	271.2653
	20	310.0239	374.683	324.5667	250.4457
	25	569.2888	452.3076	469.2662	497.2072
Zone-6: Phase b	5	104.7985	128.8168	164.0042	120.6892
	10	190.4917	149.4466	134.8459	137.1325
	15	171.6198	158.6567	190.097	180.7123
	20	270.3092	244.7032	195.9436	186.5358
	25	308.7939	336.5116	247.2021	238.5889
Zone-6: Phase c	5	119.6787	137.403	165.1748	129.3649
	10	185.7285	147.3814	140.9089	134.4484
	15	168.5095	158.5218	185.2016	172.2422
	20	254.5742	231.4679	196.2573	189.7845
	25	312.7276	348.5701	248.339	242.7853
Zone-7: Phase a	4	278.0128	194.5997	161.7302	136.9156
	8	242.1587	155.9738	99.49957	120.2239
	12	244.2018	216.4986	137.322	125.3612
	16	184.5326	191.2894	201.3837	195.461
	20	192.6291	256.2483	249.8618	166.0997
Zone-7: Phase a	4	141.53	125.3897	85.27911	70.59581
	8	99.79442	113.4803	81.65146	86.89787
	12	167.7856	128.9359	119.7982	86.10992
	16	188.6617	162.9766	145.5651	127.8336
	20	116.9862	163.2054	117.2235	130.4735
Zone-7: Phase a	4	142.0019	121.6928	85.24108	80.73674
	8	93.55404	112.1002	84.97488	85.07737
	12	170.7214	129.9813	119.1516	90.27449
	16	185.6097	155.0026	145.6415	135.3789

(continued)

Table 3 (continued)

FIA		20°	40°	60°	80°
Zones/Phases	Distance (km)				
	20	123.6192	166.6737	119.1306	142.1886
Zone-8: Phase a	4	1262.262	914.7941	1040.59	876.7483
	8	633.5293	633.4484	484.4508	478.497
	12	270.7869	274.7676	287.1616	269.3898
	16	372.8416	299.9607	187.8446	148.8582
	20	253.2181	258.3597	161.5231	250.8802
Zone-8: Phase b	4	738.9016	673.0562	616.0363	555.1654
	8	392.3671	290.8112	294.6176	266.7699
	12	128.0366	146.1465	145.7985	137.6743
	16	215.2371	177.3551	121.2848	111.7129
	20	148.8235	146.2723	135.7855	112.5016
Zone-8: Phase c	4	735.027	674.8348	610.1455	546.1279
	8	396.8299	295.9845	306.9234	264.4856
	12	132.1732	153.2031	152.1422	140.4799
	16	219.4116	181.2726	128.3871	117.422
	20	128.1035	130.2623	131.6589	105.929
Zone-9: Phase a	2	132.6797	103.8587	70.43439	82.68666
	4	126.2682	146.5265	116.1063	105.7688
	6	137.5003	128.1309	137.8318	94.23266
	8	117.4956	131.7681	121.1288	96.63817
	10	205.9835	103.1875	156.1563	119.3873
Zone-9: Phase b	2	50.86305	48.82548	42.18174	32.93884
	4	65.52933	63.07304	89.25785	64.62524
	6	107.8587	83.47089	79.89563	73.69413
	8	86.14352	84.50055	81.96124	71.09258
	10	92.11515	84.19993	81.10193	61.95255
Zone-9: Phase c	2	47.86158	48.32959	42.6038	30.40071
	4	67.15565	65.79728	89.63213	61.88395
	6	105.6843	82.48872	80.09079	70.90748
	8	83.99967	82.97947	82.16567	72.39437
	10	88.53601	81.7753	76.01193	62.87167

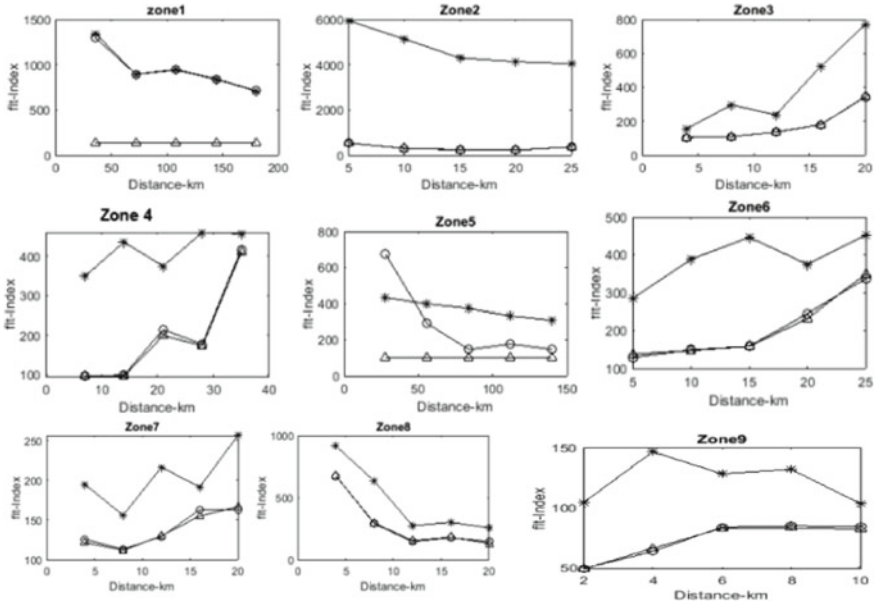

Fig. 3 Variation of fault index in all the zones without UPFC and AG fault in zone-2

is evident that coefficients are high in Zone-2 in phase A. The impact of Fault in Zone-2 is high, coefficients are high for phase A, Hence the fault is of LG type.

From Fig. 3 it clearly represents that the Fault Index value is high for Zone-2 and for Phase A. The compensation of fault can be partly achieved by connecting UPFC in between Zone-2 and Zone-3. Wavelet multiresolution analysis is performed by connecting UPFC between zone-2 and zone-3. The coefficients are taken at all the zones and buses. Loads 1, 2, 3, 4 & 5 are connected at Primaries side of DG's 1, 2, 3, and 4, which are not actually shown in one line diagram.

The compensation of fault current at Zone-2 has been shown clearly. For example, the detailed coefficient vale for AG fault at Zone-2 is at 800 is 6243.144, whereas its value is compensated to 4539.152. Thus UPFC has a considerable effect on Zone-2. Similarly, the coefficients during LG fault at FIA of 20° and at a distance of 5 km are at phase A, phase B, Phase C is 5325.777, 602.9014, 609.057, which shows this value is highest in Phase A. Therefore, it is an LG Fault (Fig. 4).

Figure 5 represents three variations of fault index due to LG Fault in Zone-2 without connecting UPFC. For understanding purpose variation of index values at Bus-1, 2, 3, and 7 have been shown. One phase current got increased much, which can be observed from the diagram.

For understanding purpose variation of index values at Bus-1, 2, 3, and 7 have been shown. Two-phase currents got increased much, which can be observed from Fig. 6 (Fig. 7).

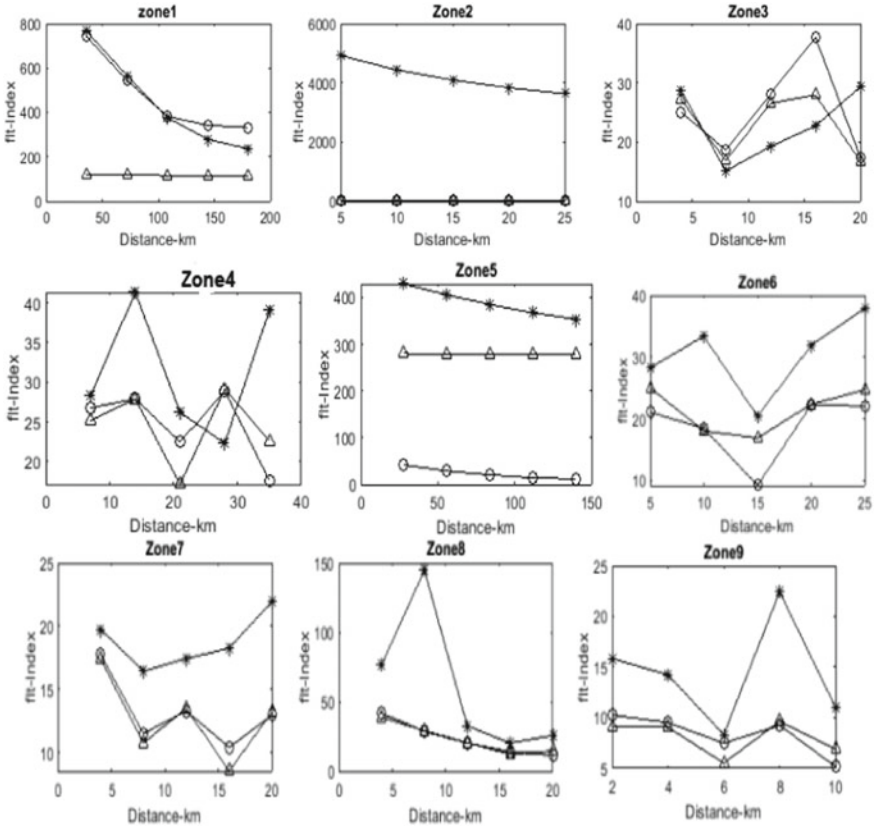

Fig. 4 Variation of fault index in different zones with UPFC and AG fault in zone-2

Figure 8 represents three the phase variations of fault index due to LLG Fault in Zone-2 with connecting UPFC. For understanding purpose variation of index values at Bus-1, 2, 3, and 7 have been shown. Two-phase currents index values variation at different buses has been analyzed, which can be observed from the diagram (Table 4).

Table 5 represents with the sum of detailed coefficients with LLLG in Zone-6, which clearly shows the impact of three-phase fault in Zone-6, the coefficients got increased. As UPFC is connected between Zone-2 and Zone-3, it has an impact on all the zones. The impact of UPFC on Zone-6 due to LLLG fault on Zone-6 can be tabulated in Table 4 (Table 6).

The impact also can be seen for different angles i.e., Fault inception angles. For understanding purposes, only one zone has been shown. Figure 10 represents the impact of UPFC on Zone-6 and Zone-7. From the above figures and tables, It is evident that interconnected networks there is an impact of fault in any Zone reflects fault current on other zones also. At the initial stage by applying fault at each zone, analyzed the detailed coefficients. The fault impact is high in the zone where the fault occurs, whereas there is an impact on other zones. This paper uses UPFC as a

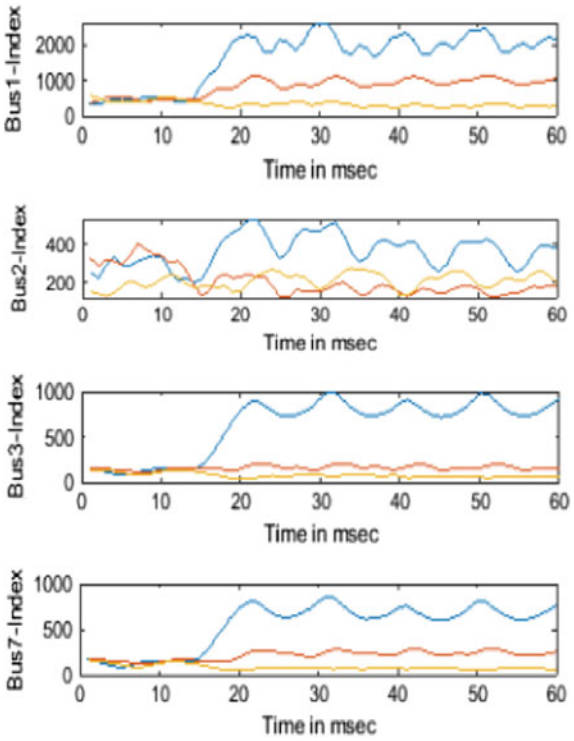

Fig. 5 Variation of fault index at buses 1, 2, 3, 7 due to LG fault in zone-2 without UPFC

Fig. 6 Represents three variation of fault index due to LLG fault in zone-2 without connecting UPFC

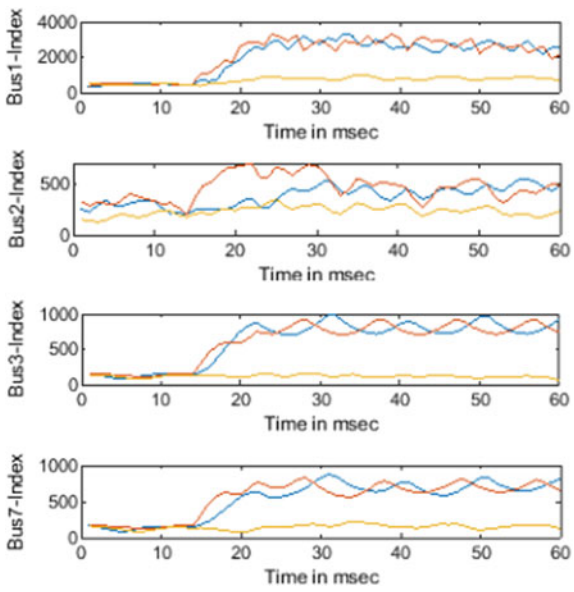

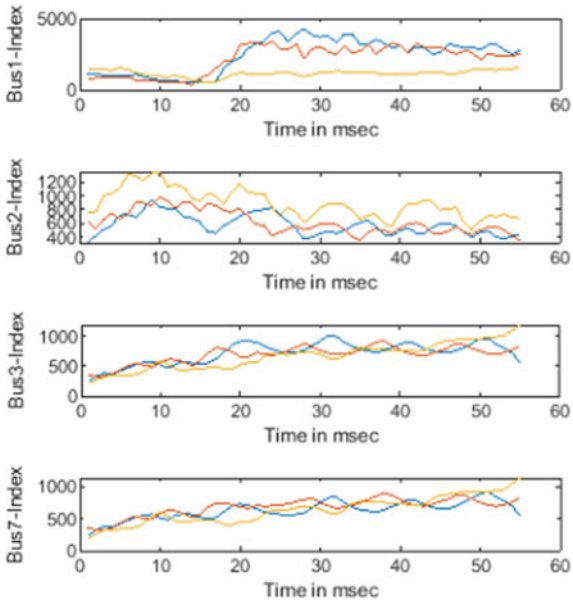

Fig. 7 Variation of fault index at bus 3, 7 due to LLG fault in zone-2 with UPFC

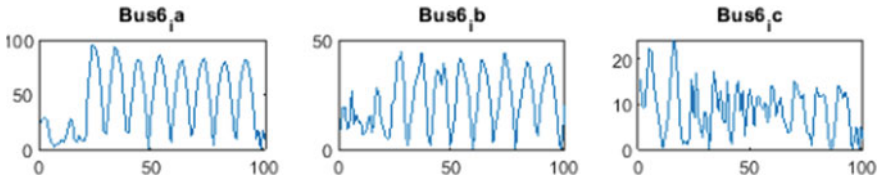

Fig. 8 Variation of effective coefficients of LG fault in zone-2 from terminal-6

compensating device. Even though UPFC is connected between Zone-2 and Zone-3. The fault currents are compensated up to a certain limit, therefore fault current has an impact on other zones too in presence of UPFC (Figs. 9 and 10).

6 Conclusions

The evaluation of dynamic behavior during transient conditions has been studied for multiterminal network. Wavelet analysis will give the entire system performance at any part of the system. This paper mainly concentrates on fault detection and its classification of multiterminal networks. It also gives a critical evaluation of nine zones of performance under different fault conditions. The performance of multiterminal transmission networks with and without UPFC under different fault conditions has been estimated. This algorithm successfully analyzed the different

Table 4 LG Fault on Transmission line in Zone-2 with UPFC

FIA		20°	40°	60°	80°
Zone-s/Phases	Distance (km)				
Zone-2: Phase a	5	4091.516	4920.359	5305.573	4539.152
	10	3914.136	4437.367	4778.623	4298.473
	15	3655.694	4091.654	4365.893	3974.26
	20	3404.021	3831.482	4033.917	3669.852
	25	3210.693	3636.321	3784.54	3429.58
Zone-2: Phase b	5	49.24836	35.88597	23.73107	25.81357
	10	30.64287	29.26032	22.79283	20.67209
	15	24.35378	17.32852	12.20013	18.5182
	20	62.90602	43.49543	42.31739	33.72605
	25	21.96338	19.1193	13.27504	15.52662
Zone-2: Phase c	5	47.61342	30.67786	30.75633	31.71313
	10	36.30296	28.69022	27.67097	23.68694
	15	21.05736	16.59344	19.5321	19.12578
	20	58.38437	42.06938	44.91864	34.02227
	25	21.49128	11.32597	15.00123	15.51111

Table 5 LLLG Fault on Transmission line in Zone-6 without UPFC

FIA		20°	40°	60°	80°
Zone-s/Phases	Distance (km)				
Zone-6: Phase a	5	3796.282	4681.449	5474.372	4144.664
	10	4824.178	4738.143	4644.604	4811.901
	15	4561.506	4749.508	4678.542	5166.384
	20	4307.706	5037.11	4611.306	4993.97
	25	4203.645	4586.955	4725.963	4972.756
Zone-6: Phase b	5	5134.595	4438.365	3978.692	3829.604
	10	5167.076	4423.533	3856.865	3841.574
	15	5185.629	4470.881	3921.195	3926.038
	20	5243.934	4500.099	3981.756	3971.895
	25	5291.249	4555.34	4030.181	3991.938
Zone-6: Phase c	5	3696.025	3339.338	3293.723	4253.44
	10	3879.838	2596.72	4352.824	4199.134
	15	4545.749	3553.078	5023.077	4540.078
	20	4572.546	4135.908	5219.165	4567.857
	25	4640.83	3900.611	4771.929	4486.894

Table 6 LLLG Fault on Transmission line in Zone-6 with UPFC

FIA		20°	40°	60°	80°
Zone-s/Phases	Distance (km)				
Zone-6: Phase a	5	3531.738	4833.433	4906.147	4210.159
	10	3522.45	4771.164	4840.717	4206.845
	15	2920.681	4001.9	4301.455	3937.241
	20	2776.039	3269.824	3662.967	3705.497
	25	2839.302	3291.158	3679.335	3702.119
Zone-6: Phase b	5	4699.737	4061.111	4130.061	3760.77
	10	4633.304	3947.565	4114.084	3749.02
	15	4725.281	3990.008	4126.915	3714.14
	20	5060.88	4217.889	4246.952	3660.499
	25	5447.277	4487.549	4430.945	3714.135
Zone-6: Phase c	5	2631.14	2913.362	4101.797	4427.076
	10	2933.219	2947.628	4327.078	4594.922
	15	3330.649	3040.203	4026.577	3976.125
	20	4252.276	3195.382	3713.94	3083.504
	25	5095.979	3896.149	4361.107	3567.025

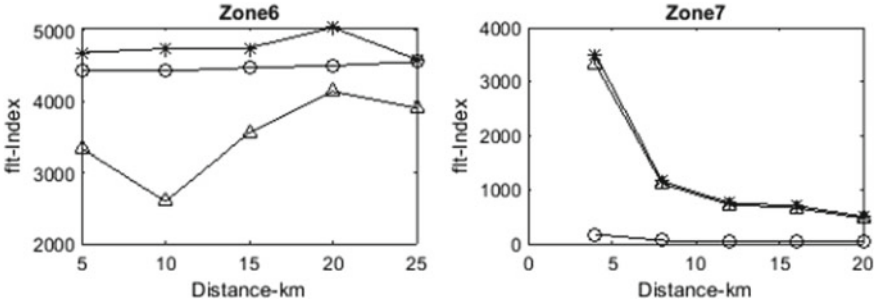

Fig. 9 Variation of fault index LLLG fault in zone-6 without UPFC

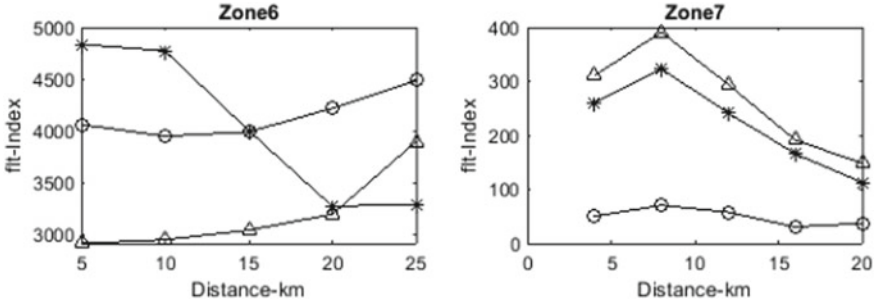

Fig. 10 Variation of fault index LLLG fault in zone-6 with UPFC

faults in all the zones. The proposed scheme is fast and accurate. Even it performs well at different fault inception angles. The effectiveness of the system is obtained by connecting UPFC between Zone-2 and Zone-3 has been evaluated more effectively. Wavelet-based multiresolution analysis is applied to multiterminal interconnected networks. Bior 1.5 is chosen as mother wavelet.

References

1. Sadeh J, Adinehzadeh A (2010) Accurate fault location algorithm for transmission line in the presence of series connected FACTS devices. Int J Elect Power Energy Syst 32:323–328
2. Samantaray SR, Dash PK, Upadhyay SK (2009) Adaptive Kalman filter and neural network based high impedance fault detection in power distribution networks. Int J Elect Power Energy Syst 31:167–172
3. Samantray SR, Dash PK (2008) Pattern recognition based digital relaying for advanced series compensated line. Int J Elect Power Energy Syst 30:102–212
4. Suja S, Jerome J (2010) Pattern recognition of power signal disturbances using S Transform and TT Transform. Int J Elect Power Energy Syst 32:37–53
5. He Z, Gao S, Chen X, Zhang J, Bo Z, Qian Q (2011) Study of a new method for power system transients classification based on wavelet entropy and neural network. Int J Elect Power Energy Syst 33:402–410
6. Pardha Saradhi J, Srinivasa Rao R, Ganesh V (2019) Wavelet based power quality assessment of wind energy source integrated 5-bus system under sudden load conditions in presence of FACTS devices. Int J Eng Adv Technol (IJEAT) 8(6S3). ISSN: 2249-8958
7. Goli RK, Shaik AG, Tulasi Ram SS (2015) A transient current based double line transmission system protection using fuzzy-wavelet approach in the presence of UPFC. Electr Power Energy Syst 70:91–98
8. El-Zonkoly AM (2011) Wavelet entropy based algorithm for fault detection and classification in FACTS compensated transmission line. Electr Power Energy Syst 33:1368–1374
9. Biswajit Sahoo SR, Samantaray (2018) Wavelet-based auto-reclosing technique for TSC compensated lines connecting wind farm, IEEE